Clays and Clay Minerals, Vol. 40, No. 5, 531–539, 1992.

INFLUENCE OF Fe(II) ON THE FORMATION OF THE SPINEL IRON OXIDE IN ALKALINE MEDIUM

J. P. JOLIVET, P. BELLEVILLE, E. TRONC, AND J. LIVAGE
Chimie de la Matière Condensée (CNRS URA 1466)
Université Pierre et Marie Curie, Paris 05, France

Abstract—Fe(II) and Fe(III) in various proportions were coprecipitated by NH_3 at pH ≈ 11. The Fe(II)/Fe(III) ratio (x) was varied from 0.10 to 0.50. After stabilization by aging at pH ≃ 8 in anaerobic conditions, hydrous precipitates were characterized by electron microscopy, Mössbauer spectroscopy, and kinetics of dissolution in acidic medium. At any x value, all stable products exhibited the structure of (oxidized) magnetite. For $x \leq 0.30$, two distinct species were coexisting: the one ("m") was made up of ca. 4nm-sized particles with a low Fe(II) content (Fe(II)/Fe(III) ≈ 0.07), and the other ("M") consisted of particles of larger, more or less distributed sizes, and composition Fe(II)/Fe(III) ≈ 0.33; "M" increased relative amount with increasing x. For $x \geq 0.35$, "M" was the only constituent and its Fe(II)/Fe(III) ratio was equal to x. "M" is identified with (nonstoichiometric) magnetite, whereas "m" is likely to be an oxyhydroxide. Mechanisms of formation are discussed, and a phase diagram is proposed which schematizes the evolution of the coprecipitation products with x and with time. Addition of Fe(II) after the precipitation of Fe(III), instead of coprecipitation, yielded very similar results.

Key Words—Dissolution, Ferrihydrite, Maghemite, Magnetite, Mössbauer spectroscopy.

INTRODUCTION

Divalent transition metal cations (M = Fe, Mn, Cu, Ni, Co, Zn) at sufficiently high ratios (M(II)/Fe(III) > 0.2, roughly) are known to interact with the least ordered variety of ferrihydrite to produce phases with the spinel structure (Cornell and Giovanoli, 1987, 1988; Cornell, 1988; Mann *et al.*, 1989). This generally proceeds by dissolution and reprecipitation.

We recently reported (Tronc *et al.*, 1992) that Fe(II) ions in alkaline medium (pH ≈ 11) can also make ferrihydrite convert to a spinel phase by a reaction in the solid state. Fe(II) adsorption induces an interfacial electron transfer and the mobility of the extra electrons within the whole Fe(II)-ferrihydrite particle drives the transformation. The rearrangements required for electron hopping occur easily because of the low degree of cross linking in ferrihydrite. They proceed by olation/oxolation processes with water elimination. At any value of the Fe(II)/Fe(III) ratio (x), local ccp ordering rapidly sets in; the degree of ordering increases with x and with time. The reaction is competing with dissolution of complexes from the surface; the Fe(II) level rules the kinetics of the two processes and the composition of the soluble species. At $x < 0.1$, the ordering remains globally too poor to ensure stability against dissolution. The dissolved species have a low Fe(II) content and recrystallize into goethite, the only stable phase. Pure ferrihydrite, too, converts into goethite in the experimental conditions, with the presence of Fe(II) ions accelerating the conversion. A similar effect also occurs at pH 5–7 (Fischer, 1973). At $x > 0.1$ (Tronc *et al.*, 1992), goethite formation is totally suppressed and both reactions, in the solid state and via the solution, lead to stable (nonstoichiometric) magnetites which can be morphologically very distinct.

In this paper we report an investigation of these magnetites as a function of the initial Fe(II) level ($0.10 < x \leq 0.50$). The materials were obtained by simultaneous or successive precipitation of Fe(III) and Fe(II) ions in alkaline medium, and aging in anaerobic conditions at pH ≈ 8 and room temperature for 1–2 days. Hydrous materials were characterized by electron microscopy, dissolution kinetics in acidic medium, and Mössbauer spectroscopy.

EXPERIMENTAL METHODS

Materials

Aqueous mixtures of $FeCl_3$ (40 cm^3, 1 M) and $FeCl_2$ (2 M, 2 M HCl) in various proportions were added to an NH_3 solution (400 cm^3, 0.6 M, pH ≈ 11) with vigorous stirring at room temperature. A dark brown precipitate instantaneously formed. The solid was separated by magnetic settling on a permanent magnet (or by centrifuging), washed with degassed distilled water, separated again, redispersed in distilled water, and stored under argon. The pH of the suspensions was near 8 and the Fe concentration was about 0.1 M. All preparation and separation steps were carried out using degassed solutions and nitrogen flowing within the vessel. The Fe(II)/Fe(III) molar ratio (x) in the initial mixture was varied from 0.10 to 0.50. At $x = 0.15$ and 0.50, experiments were also carried out with addition of Fe(II) after the precipitation of Fe(III).

Methods

Chemical analysis. Fe(II) and total Fe concentrations in the suspensions were determined after dissolving the solid in concentrated HCl. Fe(II) was titrated potentiometrically with $K_2Cr_2O_7$. At the titration end, in order to determine the total Fe concentration, all Fe ions were reduced with a $SnCl_2$ solution, and the mixture was again titrated with $K_2Cr_2O_7$.

Chemical reactivity. The various solid species were characterized by their kinetics of dissolution in acidic medium (2 M HCl). The dissolution frees both Fe(II) and Fe(III) species. As they were released into solution, Fe(III) species were reduced by KI (0.2 M). The liberated I_2 was automatically titrated with $Na_2S_2O_3$ ions using a 3D Metrohm Combititreur which maintained the potential in the medium at the equivalent point of the $I_2/S_2O_3^{2-}$ redox reaction. This method left no excess iodine in the medium, and I^- concentration remained constant during the dissolution. Because of acid excess, H^+ concentration was quasi constant. The two reduction reactions (Fe(III)/I^- and $I_2/S_2O_3^{2-}$) are very fast so that the rate of the global reaction is determined by the dissolution of the particles. Data analysis using pseudo-first-order rate laws yielded dissolution rate constants and proportions of the various Fe(III) species.

Suspension fractionation. In some cases, suspended particles were separated according to their size. The separation was carried out entirely under flowing Ar. The suspension was magnetically concentrated and the supernatant liquid (free of Fe) was eliminated. The solid was treated with concentrated $N(CH_3)_4OH$. The mixture was vigorously stirred and magnetically settled. The supernatant sol (Jolivet *et al.,* 1983) was isolated. It contained the smallest particles and constitutes the small particle size fraction hereafter termed the S-fraction. The settled fraction was washed alternatively with water and $N(CH_3)_4OH$ until magnetic settling yielded a supernatant free from colloids. The solid was dispersed in water in an Ar atmosphere. This fraction made up of particles of large size was termed the L-fraction.

Techniques

Transmission electron microscopy. Micrographs and diffraction patterns were obtained on a JEOL 100 CXII apparatus. Samples were prepared by evaporating very dilute ultrasonicated solutions onto carbon-coated grids. The d-spacings were calibrated using a Au pattern. Particle size distributions were estimated by measuring the size of about 400 particles.

Mössbauer spectrometry. Mössbauer spectra were recorded using a conventional spectrometer (ELSCINT-INEL) with a $^{57}Co/Rh$ source. The suspensions were added to an aqueous solution of polyvinyl alcohol and the mixtures were dried in an Ar flow yielding rigid films. Some samples consisted in suspensions confined in a plastic cell, rapidly frozen to 77K. Velocities were calibrated using an iron foil. Isomer shifts are given relative to metallic iron at room temperature.

RESULTS

The following results generally concern suspensions aged for 1 or 2 days. Their composition always corresponded to the stoichiometry of the initial Fe(II)/Fe(III) mixture. Operating conditions effectively avoided oxidation. The addition of Fe(II) after the precipitation of Fe(III) yielded the same features as coprecipitation, as reported earlier (Tronc *et al.,* 1992).

Influence of the level of Fe(II)

Electron microscopy. Images of hydrous precipitates at $x = 0.10$–0.15 showed two distinct types of particles (Figure 1a): spheroids of ca. 4 nm and well-faceted prismatic crystallites of 25 to 150 nm. Selected area diffraction (Figures 1b and 1c) showed that particles of each type had the spinel structure. The large crystallites generally yielded diffuse scattering features indicative of stacking faults. With increasing x (Figure 1d), the large particles became less numerous and smaller, while the small particles significantly increased in size. Above $x = 0.25$, no particle larger than 20 nm was observed and the system appeared to be made up of a single type of particle whose mean size increased with x (Figures 1e and 1f). Size distributions are shown in Figure 2, other data are given in Table 1. Size distributions for $x < 0.25$ samples only concern the small particles; because of the very large difference in the size of the "small" and "large" particles, the two populations could not be correlated on the same diagram.

Observations performed after prolonged storage showed that the suspensions at $x > 0.10$ remained practically unaltered even after several months. After 8 days, the suspension at $x = 0.10$ contained a few crystallites of goethite and hematite and only small changes occurred with further aging.

Mössbauer spectroscopy. At room temperature, the spectrum of magnetite consists of two sextets. One (B) is due to the Fe(II) and Fe(III) ions paired by electron exchange in octahedral sites, and the other (A) to the Fe(III) ions in tetrahedral sites. The unpaired Fe(III) octahedral ions in partly oxidized magnetite contribute to the A subpattern (Daniels and Rosencwaig, 1969) so that the B/A area ratio decreases from 2, approximately, down to 0 with increasing oxidation. Generally, particles more than 10 nm in size give the bulk pattern with hyperfine fields reduced by collective magnetic excitations. Particles smaller than 6 nm are superparamagnetic and produce a paramagnetic pattern. Intermediate sizes lead to complex spectra (Mørup *et*

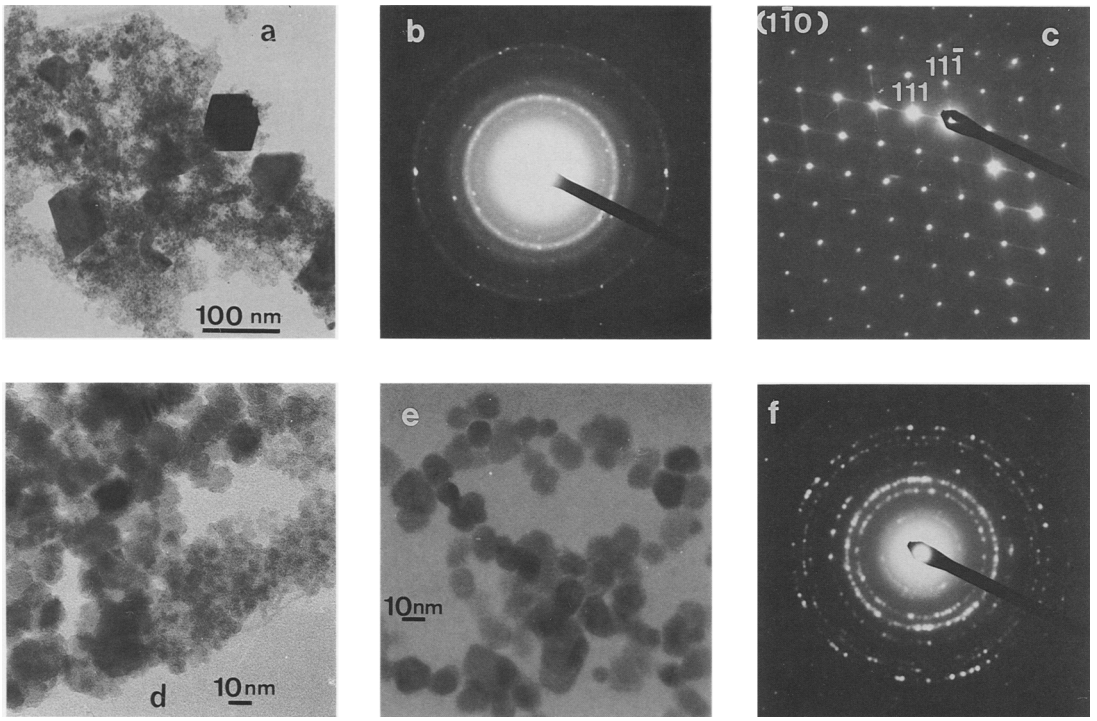

Figure 1. Electron microscopy observations from precipitates formed at various Fe(II)/Fe(III) ratios (x), aged for 1–2 days. For (a), (b), and (c) x = 0.15, image and selected area diffraction from small particles and a crystal, respectively; (d) x = 0.25; (e) and (f) x = 0.50.

al., 1976, 1980; Coey and Khalafalla, 1972; Tronc and Bonnin, 1985).

The spectra of the precipitates at x = 0.10–0.15 show the magnetite pattern superimposed on a symmetrical doublet (Figure 3). With increasing x, the magnetite pattern grows at the expense of the doublet, and for x = 0.50 the spectrum is similar to that of 10-nm Fe_3O_4 particles (Mørup *et al.*, 1976). Mössbauer parameters were determined by fitting the spectra to simple distributions with 2 or 3 hyperfine fields for each of the 2 magnetite subpatterns. The quadrupole shifts were fixed at zero and the line widths of the various sextets were constrained to be all equal. Overall departure from the theoretical 3:2:1 intensity ratio was allowed. The parameters obtained from these fits are given in Table 2.

The A and B isomer shifts identical to those of bulk magnetite (Murad and Johnston, 1987), and the hyperfine fields reduced in similar proportions are consistent with the size effect (Figures 2 and 7a). The a_B/a_A area ratios, generally much smaller than 2, are typical of nonstoichiometric magnetite. Their variation suggests a break in the evolution of the composition. The ratio of the recoilless fractions of ^{57}Fe nuclei in octahedral (o) and tetrahedral (t) sites in Fe_3O_4 at room temperature is $f_o/f_t = 0.94$ (Sawatzky *et al.*, 1969). For nearly stoichiometric materials Fe(II)/Fe(III) $\approx a_B/(1.88\ a_A + a_B)$, which yields Fe(II)/Fe(III) = 0.48 for the x = 0.50 material, in good agreement with the theoretical value. However, in the case of significant oxidation, because of mixed Fe_o and Fe_t contributions to the A pattern, it is simpler to assume the same recoilless fraction for all Fe ions; then Fe(II)/Fe(III) $= a_B/(2\ a_A + a_B)$. Thus, the data suggest that Fe(II)/Fe(III) = 1/3 for $x \leq 1/3$, and Fe(II)/Fe(III) = x for $x \geq 1/3$.

The paramagnetic pattern only exists for $x < 0.35$. It shows no resolved Fe(II) ($Fe^{2.5+}$) component and the parameters are typical of Fe(III) ions in small iron oxide particles (Tronc and Bonnin, 1985; Murad and Schwertmann, 1980; Murad and Johnston, 1987).

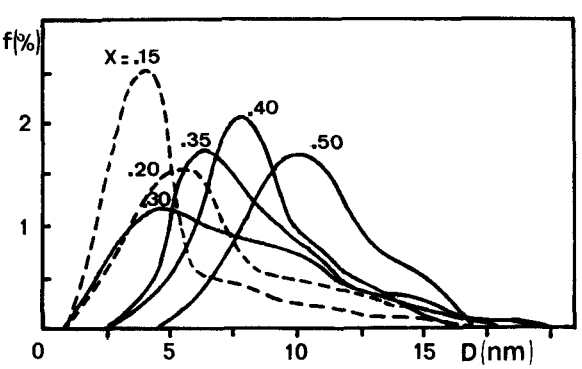

Figure 2. Particle size distributions as a function of the initial Fe(II)/Fe(III) ratio (x); (– – –) truncated distributions (see text).

https://doi.org/10.1346/CCMN.1992.0400506 Published online by Cambridge University Press

Table 1. Characteristics of suspensions formed at various Fe(II)/Fe(III) ratios (x), and aged for 1–2 days.

x	0.10	0.15	*0.15*	0.20	0.25	0.30	0.35	0.40	0.45	0.50	*0.50*
D (nm)	–	5.2[1]	*5.4*[1]	7.2[1]	–	7.5	8.5	8.6	10.2	10.6	*10.5*
σ (nm)	–	3.1	*3.1*	3.7	–	3.7	3.1	2.5	2.8	2.4	*2.5*
Immediately dissolved											
f (%)	10	5	*6*	3	7						
k_1 (min^{-1})	0.51	0.40	*0.38*	0.45	*						
f (%)	73	65	*66*	52	25						
k_2 (min^{-1})	0.012	0.012	*0.018*	0.026	0.044	0.055	0.090	0.096	0.100	0.120	*0.110*
f (%)	17	30	*28*	45	68	100	100	100	100	100	*100*

Data in italics refer to successive precipitation, others to coprecipitation. D and σ stand for mean and standard deviation of size distributions, respectively; [1] truncated distribution as mentioned in the text; k_1 and k_2 are dissolution rate constants; f is the fraction of dissolved Fe(III); * not determined.

Therefore, the Fe(II)/Fe(III) ratio must be low in the (super)paramagnetic fraction (≈0.1 with the above assumption), and a mixture of superparamagnetic oxidized magnetite and ferrihydrite cannot *a priori* be excluded. Note that this cannot be confirmed or excluded by TEM observations owing to the very small size of the particles and poor structural ordering of ferrihydrite.

Dissolution kinetics. Ferrihydrite dissolves quasi-instantaneously at the pH conditions used, while magnetite dissolves more slowly regardless of the particle

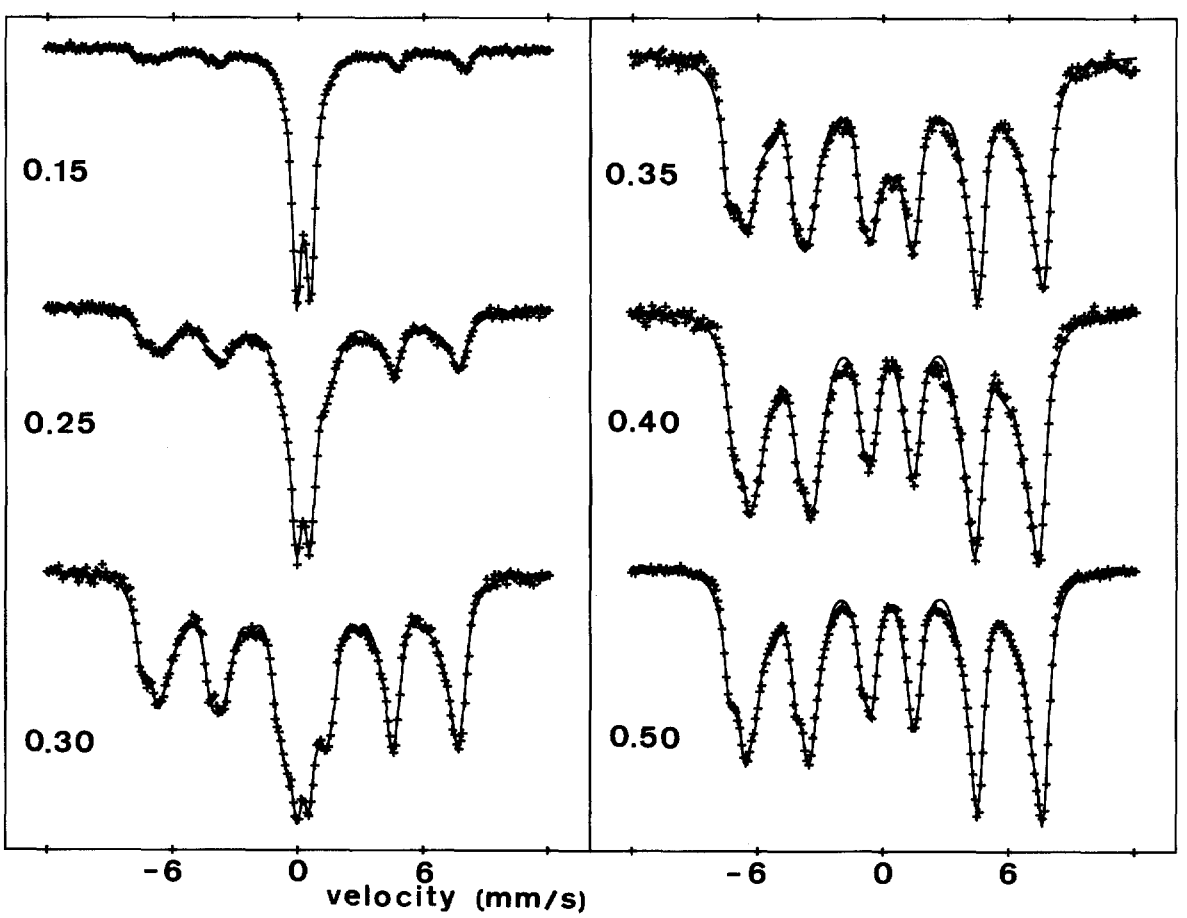

Figure 3. Observed and calculated Mössbauer spectra (295 K) of frozen in suspensions of different Fe(II)/Fe(III) compositions.

https://doi.org/10.1346/CCMN.1992.0400506 Published online by Cambridge University Press

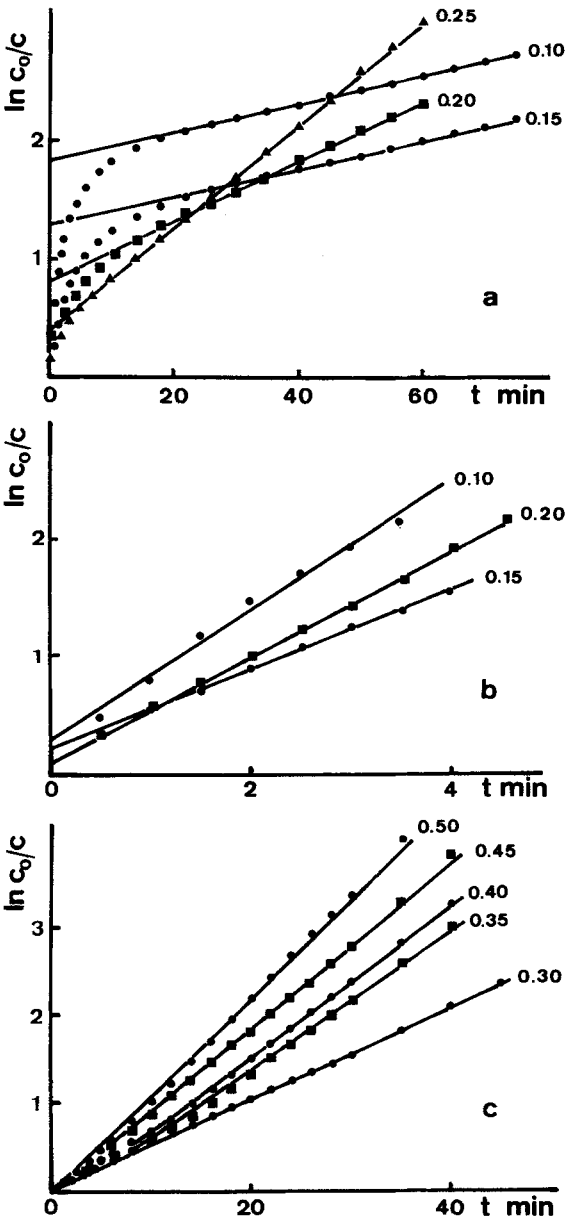

Figure 4. Dissolution kinetics for suspensions of various Fe(II)/Fe(III) stoichiometries (x). (a) $x \leq 0.25$; (c) $x \geq 0.30$; (b) plot of the first stages appearing in (a), recalculated by taking into account the amount of slowly dissolved species determined by extrapolation in (a). (c_0 represents the amount of total Fe(III) and c represents Fe(III) undissolved at time t). Straight lines correspond to first-order rate law fits.

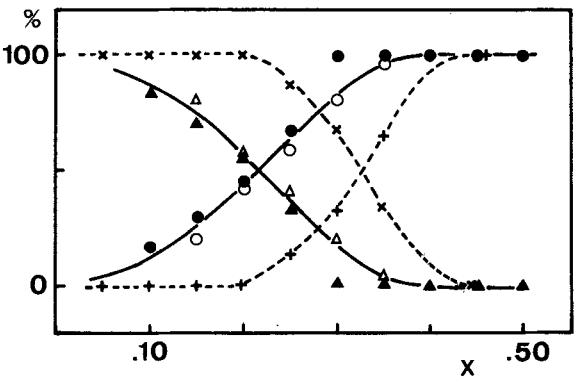

Figure 5. Suspension constitution as a function of the Fe(II)/Fe(III) ratio. Fe(III) partitioning in early systems (– – –), data taken from Tronc *et al.*, 1992: Fe(II)-ferrihydrite (×), and magnetite (+). In aged systems (——) as deduced from Mössbauer and dissolution kinetics data: (super)paramagnetic (△) and magnetic (○) fractions, immediately plus rapidly (▲) and slowly (●) dissolved species.

size and the Fe(II)/Fe(III) ratio (Tronc *et al.*, 1992). Small particles of magnetite and ferrihydrite can thus be differentiated by the rate of dissolution.

Dissolution rate results (Figure 4, Table I) exhibit two types of behavior depending upon the x value. At $x < 0.30$ (Figures 4a and 4b) there are three distinct stages corresponding to immediate, rapid (rate constant k_1), and slow (k_2) dissolution, successively. As x increases, k_1 remains practically constant and k_2 regularly increases. At $x \geq 0.30$ (Figure 4c) the stage of immediate dissolution no longer exists and there is practically only one kinetic stage. The rate constant (k_2) jumps between $x = 0.30$ and 0.35, then slightly increases up to $x = 0.50$. Ferrihydrite is present only for $x < 0.30$, and then only in small quantities ($\leq 10\%$ of total Fe(III)).

The characteristics of the dissolution of the magnetite particles vary strongly with x. This is due to size and/or composition effects. Comparing the Fe(III) partitioning with that deduced from Mössbauer data (Figure 5), it appears that rate constant k_1 is to be associated with the superparamagnetic particles, and k_2 with the magnetically blocked ones. The difference between k_1 and k_2 is mainly due to the size effect. As x increases from 0.15 to 0.30, the Fe(II)/Fe(III) ratio in the large particles remains constant (Table 2) while their mean size decreases (Figure 2) making k_2 increase. From $x = 0.35$ up to 0.50, k_2 and the mean size both increase, which is not consistent with a pure size effect. The increase in the Fe(II)/Fe(III) ratio in the particles is likely to have the dominant effect. The fact that an increase in the Fe(II) level enhances the dissolution in acidic medium may be related to the release of iron as Fe(II) exclusively in weakly acidic medium (Jolivet and Tronc, 1988). Both phenomena are likely to be connected with the high mobility of electrons in the octahedral sublattice.

Analysis of fractionated suspensions

The species formed at low x values were characterized separately by fractionating the $x = 0.15$ sample. The small (S) and large (L) particle fractions showed a mean particle size of 4 nm and 57.5 nm (Figures 6 and

https://doi.org/10.1346/CCMN.1992.0400506 Published online by Cambridge University Press

Table 2. Mössbauer parameters (295 K) of the coprecipitation products as a function of the initial Fe(II)/Fe(III) ratio (x).

x	0.15	0.20	0.25	0.30	0.35	0.40	0.50
IS	0.33(1)	0.33(1)	0.33(1)	0.34(1)	0.35(2)	—	—
QS	0.66(1)	0.66(1)	0.65(1)	0.56(1)	0.40(5)	—	—
W	0.58(1)	0.62(1)	0.70(1)	0.70(2)	0.70(2)	—	—
a (%)	78	56	38	16	4	—	—
A: IS	0.31(2)	0.26(2)	0.25(2)	0.21(1)	0.23(1)	0.26(1)	0.25(1)
H_m	48.3(2)	47.6(2)	46.5(2)	46.9(1)	46.6(1)	45.2(1)	46.3(2)
⟨H⟩	47.0	46.1	44.8	42.4	42.5	42.5	44.6
a (%)	11	21	30	41	48	45	37
B: IS	0.60(2)	0.65(3)	0.65(2)	0.61(1)	0.61(2)	0.63(1)	0.62(1)
H_m	45.5(6)	45.2(2)	44.3(2)	45.2(2)	44.3(2)	43.4(1)	44.5(3)
⟨H⟩	44.8	43.3	41.8	41.0	40.8	40.9	41.3
a (%)	11	23	31	43	48	55	63

IS, QS, and W (mm/s) stand for isomer shift, quadrupole splitting, and line width, respectively. H_m and ⟨H⟩ Teslas (T) stand for most probable and mean hyperfine field, respectively. The relative absorption area is a.

7a). Chemical analysis yielded Fe(II)/Fe(III) compositions of 0.07 and 0.30, respectively.

Dissolution kinetics (Figure 7b and Table 3) show that ferrihydrite is present only in the S fraction where it represents 10% of the Fe(III). The rate constant of the major stage in the dissolution of the S fraction is equal to the rate constant k_1 involved in the dissolution of the whole suspension (Table 1). Therefore the same particles are concerned, their size is less than or about 5 nm, and their Fe(II)/Fe(III) stoichiometry is certainly less than or about 0.07. The larger particles (k_2) in the S fraction may have a higher Fe(II) content. As suggested above, dissolution behavior at rate constant k_2 in the dissolution of the whole suspension (Table 1) concerns all the particles larger than ca. 5 nm. The lack of selectivity in spite of dissolution rate decreasing by an order of magnitude when particle sizes increase from 5–10 nm (k_2, S) to ≈60 nm (k_2, L) (Table 3), probably comes from the uniform distribution of sizes over the range 5–150 nm (Figures 2 and 7a).

The temperature evolution of the Mössbauer spectrum of the S fraction (Figure 8a) is typical of superparamagnetic relaxation (Mørup *et al.*, 1980). The blocking temperature (50% of the spectral area in the superparamagnetic and magnetically split compo-

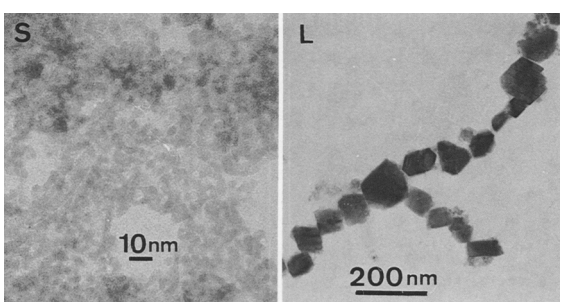

Figure 6. Electron micrographs of small (S) and large (L) particle size fractions isolated from a suspension of composition Fe(II)/Fe(III) = 0.15.

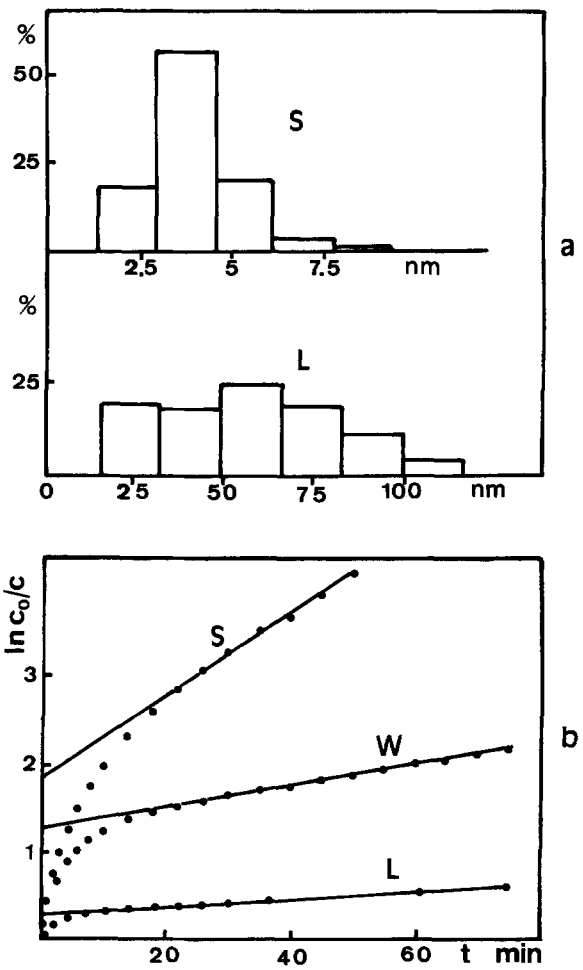

Figure 7. Characteristics of a fractionated suspension (Fe(II)/Fe(III) = 0.15). (a) Size distributions for small (S) and large (L) particle fractions; (b) dissolution kinetics for the whole suspension (W) and separated fractions (c_0 and c stand for the amounts of total Fe(III) and Fe(III) undissolved at time t, respectively).

https://doi.org/10.1346/CCMN.1992.0400506 Published online by Cambridge University Press

Table 3. Characteristics of a fractionated suspension at Fe(II)/Fe(III) = 0.15.

Fraction	S		L		
Fe(II)/Fe(III)	0.07		0.30		
D (nm) σ (nm)	4.1	*1.3*	57.4	*26*	
imm. diss. *f(%)*		*10*		—	
k_1 (min^{-1}) *f(%)*	0.37	*72*	0.49	*8*	
k_2 (min^{-1}) *f(%)*	0.04	*18*	0.004	*92*	
*	t	o	t	o_1	o_2
IS (mm/s)	0.42(1)	0.49(1)	0.42(1)	0.53(1)	0.90(1)
QS (mm/s)	0	0	0	0	−0.26(1)
H(T)	49.9(1)	51.8(1)	50.8(1)	52.8(1)	48.4(1)
a (%)	*60*	*40*	*57*	*22*	*21*

D and σ stand for mean and standard deviation of size distribution, the k_i's are dissolution rate constants, and f is the fraction of dissolved Fe(III). Mössbauer parameters at 4K are represented by *. IS, QS, H, and a stand for isomer shift, quadrupole shift, hyperfine field, and relative area, respectively, with standard deviations given in brackets.

nents) is estimated to be near 60 K. The 4 K spectrum is slightly asymmetric and shows no resolved Fe(II) component. Two-sextet fits (Table 3) yield parameters similar to those of tetrahedral (t) and octahedral (o) Fe(III) ions in small γ-Fe_2O_3 particles (Haneda and Morrish, 1977). This and the much higher blocking temperature than that of pure ferrihydrite (28K) (Murad *et al.*, 1988) support the spinel structure and confirm that ferrihydrite is present only in a small amount. The area ratio (a_o/a_t = 0.67) notably deviates from the value (1.67) expected for γ-Fe_2O_3: this may be due to strongly overlapping components and size effects which persist (De Bakker *et al.*, 1990), or to variable hyperfine parameters because of incomplete ordering of the spinel structure.

Apart from a weak component that is superparamagnetic down to ca. 150 K, the L fraction spectra (Figure 8b) are typical of bulk nonstoichiometric magnetite (Daniels and Rosencwaig, 1969; Ramdani *et al.*, 1987). Assuming identical recoilless fractions for all Fe ions at 4 K, the results of the fit (Table 3) yield Fe(II)/Fe(III) = 0.27, consistent with the chemical analysis of this fraction.

Investigations of a fractionated suspension at x = 0.10 produced similar results. The L fraction Fe(II)/Fe(III) composition was still about 0.3 while the ratio for the S fraction was equal to 0.05.

DISCUSSION

All the results consistently show that the system involves two distinct stable products with the spinel structure. One product, "m," exists only if x is roughly in the range 0.10–0.33. It is made up of particles of about the same size as starting ferrihydrite (2.5–3 nm) (Tronc *et al.*, 1992). The Fe(II)/Fe(III) stoichiometry is low (≈0.07) and independent of x. The other product ("M") forms provided x ≥ 0.10. It shows different features depending on whether x is lower or higher than about 0.33. For x < 0.33 growth phenomena strongly sensitive to the x value occur, and the Fe(II)/Fe(III) stoichiometry stands close to 0.33. For x ≥ 0.33, this stoichiometry is equal to x.

The "m" and "M" products are the result of the Fe(II)-induced transformation of ferrihydrite particles through the two competing processes: dehydration and structural rearrangements in the solid state, or dissolution of complexes from the surface and recrystallization in solution (Tronc *et al.*, 1992).

At x < 0.33, "m" is formed via the solid state re-

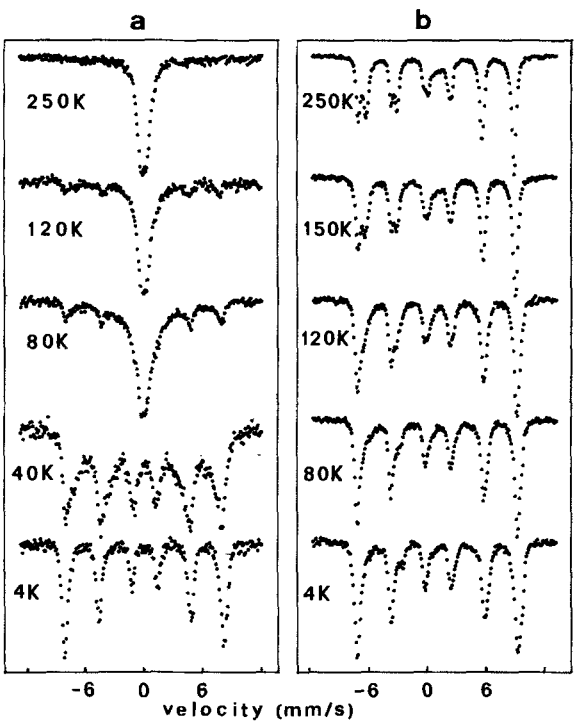

Figure 8. Mössbauer spectra of small (a) and large (b) particle size fractions isolated from a suspension of composition Fe(II)/Fe(III) = 0.15.

https://doi.org/10.1346/CCMN.1992.0400506 Published online by Cambridge University Press

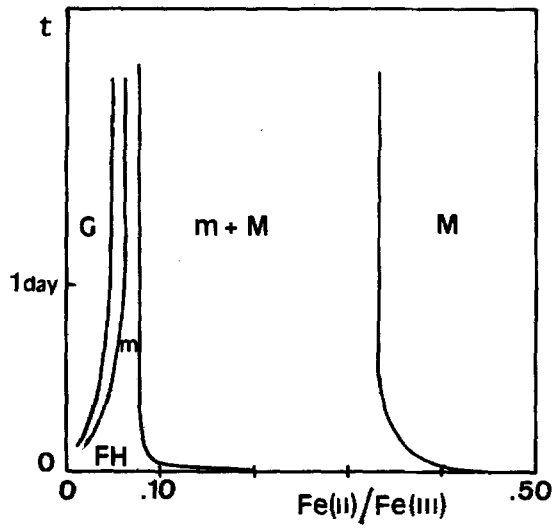

Figure 9. Phase diagram schematizing the time evolution of the products of the precipitation of Fe(III) and Fe(II) as a function of the Fe(II)/Fe(III) ratio. G and M stand for goethite and magnetite, respectively; FH stands for a ferrihydrite-like phase with variable degrees of ordering, and spinel-ordered end member m.

action and "M" exclusively grows in the solution. In view of "M" composition, the dissolved species must have a Fe(II)/Fe(III) stoichiometry close to 0.33, and crystallize as nonstoichiometric magnetite. At x = 0.10–0.15 a few "M" nuclei grow as long as complexes with suitable composition form in the solution. If x increases, more nuclei are formed and their growth is limited. The process of dissolution lowers the Fe(II) content in the small particles, the Fe(II) concentration at the surface becomes increasingly low, thus stabilizing "m" particles against dissolution.

At $x \geq 0.33$, both transformation routes lead to "M." The Fe(II) level is high enough for a very fast onset of spinel order at long range in Fe(II)-ferrihydrite particles (note that magnetite may form from the start in the case of coprecipitation). Soluble complexes of stoichiometry Fe(II)/Fe(III) $\geq$ 0.33 can form so that the particle composition is not altered by Ostwald ripening. It is likely that there are several species with Fe(II)/Fe(III) ratios in the range 0.3–0.5, and not only 0.5 (Misawa *et al.*, 1974; Tamaura *et al.*, 1981, 1983), which are able to nucleate the magnetite phase. Their structure might derive from the mixed-valence $[Fe_4O_4(OH)_2(OH_2)_{10}]^0$ species proposed by Henry *et al.* (1992), whose compact configuration, with four μ_3-oxo bridges, presumably ensures maximization of electron transfers. The magnetite formed in the present conditions, either in the solid state or via the solution, has an Fe(II)/Fe(III) ratio of at least 1/3; this minimum Fe(II) level might be related to complete dehydration of the spinel structure and/or energetic stabilization due to a cooperative effect of the mobile electrons.

In view of "m" and "M" compositions as a function of x, the system behaves like a system of two thermodynamically distinct spinel phases. The earlier reported system (Tronc *et al.*, 1992), too, behaves like a two-phase system (Figure 5). Taking into account the data relative to the time evolution at x = 0.15 (Tronc *et al.*, 1992), and considering that ferrihydrite and "m" are end members of a single phase characterized by variable degrees of hydration and structural order, we can represent the evolution of the whole system with x and time by the phase diagram in Figure 9.

"M" is an oxide and "m" is likely to be an oxyhydroxide. It exhibits all the features of the deficient spinel structure of oxidized magnetite; however, because of the process of formation, long range ordering may still be poor, significant hydroxylation is probably retained, and tetrahedral sites may be partly vacant. Pure ferrihydrite is well known to be a phase which shows variable degrees of hydration and ordering, (e.g., Chukhrov *et al.*, 1973; Eggleton and Fitzpatrick, 1988). The "m" species might actually be an additional variety, with prevailing ccp ordering. Also, this material may provide a source for finely divided maghemites in nature, independent of magnetite oxidation. At Fe(II)/Fe(III) $\leq$ 0.5, ferrihydrite converts to spinel without green rust intermediates, contrary to what is observed at higher Fe(II) levels (Mann *et al.*, 1989).

ACKNOWLEDGMENTS

We are grateful to M. Lavergne (CRMP, Université P. et M. Curie) for electron microscopy experiments.

REFERENCES

Chukhrov, F. V., Zvyagin, B. B., Gorshkov, A. I., Yermilova, L. P., and Balashova, V. V. (1973) Ferrihydrite: *Intl. Geol. Rev.* **16,** 1131–1143.

Coey, J. M. D., and Khalafalla, D. (1972) Superparamagnetic γ-Fe_2O_3: *Phys. Stat. Sol.* (a) **11,** 229–241.

Cornell, R. M. (1988) The influence of some divalent cations on the transformation of ferrihydrite to more crystalline products: *Clay Miner.* **23,** 329–332.

Cornell, R. M., and Giovanoli, R. (1987) Effect of manganese on the transformation of ferrihydrite into goethite and jacobsite in alkaline media: *Clays & Clay Minerals* **35,** 11–20.

Cornell, R. M., and Giovanoli, R. (1988) The influence of copper on the transformation of ferrihydrite ($5Fe_2O_3$, $9H_2O$) into crystalline products in alkaline media: *Polyhedron* **7,** 385–391.

Daniels, J. M., and Rosencwaig, A. (1969) Mössbauer spectroscopy of stoichiometric and nonstoichiometric magnetite: *J. Phys. Chem. Solids* **30,** 1561–1571.

De Bakker, P. M. A., De Grave, E., Vandenberghe, R. E., and Bowen, L. H. (1990) Mössbauer study of small-particle maghemite: *Hyperf. Interac.* **54,** 493–498.

Eggleton, R. A., and Fitzpatrick, R. W. (1988) New data and a revised structural model for ferrihydrite: *Clays & Clay Minerals* **36,** 111–124.

Fischer, W. R. (1973) Die Wirkung von zweiwertigem Eisen auf Lösung und Umwandlung von Eisen(III)-hydroxiden: in *Pseudogley and Gley,* E. Schlichting and U. Schwert-

mann, eds., Verlag Chemie, Trans. Comm. V and VI Int. Soc. Soil Sci., 37–44.

Haneda, K., and Morrish, A. H. (1977) On the hyperfine field of γ-Fe_2O_3 small particles: *Phys. Lett.* **64A,** 259–262.

Henry, M., Jolivet, J. P., and Livage, J. (1992) Aqueous chemistry of metal cations: Hydrolysis, condensation, and complexation: *Structure and Bonding* **77,** 154–206.

Jolivet, J. P., and Tronc, E. (1988) Interfacial electron transfer in colloidal spinel iron oxide. Conversion $Fe_3O_4 \rightarrow \gamma$-$Fe_2O_3$ in aqueous medium: *J. Colloid Interface Sci.* **125,** 688–701.

Jolivet, J. P., Massart, R., and Fruchart, J. M. (1983) Synthèse et étude physicochimique de colloïdes magnétiques non surfactés en milieu aqueux: *Nouv. J. Chim.* **7,** 325–331.

Mann, S., Sparks, N. H. C., Couling, S. B., Larcombe, M. C., and Frankel, R. B. (1989) Crystallochemical characterization of magnetic spinels prepared from aqueous solution: *J. Chem. Soc., Faraday Trans. 1* **85,** 3033–3044.

Misawa, T., Hashimoto, K., and Shimodaira, S. (1974) The mechanism of formation of iron oxides and oxyhydroxides in aqueous solutions at room temperature: *Corrosion Sci.* **14,** 131–149.

Mørup, S., Dumesic, J. A., and Topsøe, H. (1980) Magnetic microcrystals: in *Applications of Mössbauer Spectroscopy,* R. L. Cohen, ed., Academic Press, New York, **2,** 1–53.

Mørup, S., Topsøe, H., and Lipka, J. (1976) Modified theory for Mössbauer spectra of superparamagnetic particles: Application to Fe_3O_4: *J. Physique* **37,** C6 287–290.

Murad, E., Bowen, L. H., Long, G. J., and Quin, T. G. (1988) The influence of crystallinity on magnetic ordering in natural ferrihydrites: *Clay Miner.* **23,** 161–173.

Murad, E., and Johnston, J. H. (1987) Iron oxides and oxyhydroxides: *Mössbauer Spectroscopy Applied to Inorganic Chemistry,* G. J. Long, ed., Plenum Press, New York, **2,** 507–582.

Murad, E., and Schwertmann, U. (1980) The Mössbauer spectrum of ferrihydrite and its relation to those of other iron oxides: *Amer. Mineral.* **65,** 1044–1049.

Ramdani, A., Steinmetz, J., Gleitzer, C., Coey, J. M. D., and Friedt, J. M. (1987) Perturbation de l'échange électronique rapide par les lacunes cationiques dans $Fe_{3-x}O_4$ ($x \leq 0.09$): *J. Phys. Chem. Solids* **48,** 217–228.

Sawatzky, G. A., Van der Woude, F., and Morrish, A. H. (1969) Recoilless-fraction ratios for Fe^{57} in octahedral and tetrahedral sites of a spinel and a garnet: *Phys. Rev.* **183,** 383–386.

Tamaura, Y., Buduan, P. V., and Katsura, T. (1981) Studies in the oxidation of iron (II) ion during formation of Fe_3O_4 and α-FeOOH by air oxidation of $Fe(OH)_2$ suspensions: *J. Chem. Soc. Dalton Trans.* 1807–1811.

Tamaura, Y., Ito, K., and Katsura, T. (1983) Transformation of γ-FeOOH to Fe_3O_4 by adsorption of Fe(II) ion on γ-FeOOH: *J. Chem. Soc. Dalton Trans.* 189–194.

Tronc, E., and Bonnin, D. (1985) Magnetic coupling among spinel iron oxide microparticles by Mössbauer spectroscopy: *J. Physique Lett.* **46,** L437–L443.

Tronc, E., Belleville, P., Jolivet, J. P., and Livage, J. (1992) Transformation of ferric hydroxide into spinel by Fe(II) adsorption: *Langmuir* **8,** 313–319.

(Received 20 April 1992; accepted 10 September 1992; Ms. 2210)